JOURNAL OF MATERIALS SCIENCE 12 (1977) 1895–1902

Precipitation of Ni_3Al in a nickel rich NiAl

R. MOSKOVIC*
Department of Metallurgy and Materials Science, University of Cambridge, Cambridge, U.K.

A study has been made of precipitation processes occurring during ageing of NiAl martensite. The precipitation mechanism was found to be dependent on the ageing temperature, two mechanisms being observed: below ~ 700° C (the G.P. zone solvus temperature), coherent nucleation and growth of a metastable form of Ni_3Al on the microtwins inside, and interfaces between, the martensite plates was observed. In the former case, the growth of precipitates in martensite involved particle-twin interactions, which could take two forms: either a particle pushed forward the twin interface, which could bulge forward sufficiently to cut up the twins, or a growing particle developed growth twins. A model is proposed to account for these observations. In the latter case the precipitates on the martensite interfaces coarsen preferentially, leading to the formation of an equilibrium precipitate, which has an irregular rod shaped morphology.

1. Introduction

Quenching of nickel rich NiAl solid solutions is accompanied by the formation of fine plate-like precipitates on {110} as shown by Russell and Edington [1] and Moskovic [2]. So far this phenomenon has received very little further attention, although there are data in the literature which indicate that both coherent and incoherent precipitation of Ni_3Al occurs during ageing.

Arkhangel'skaya *et al.* [3] reported that in the Ni–35 at.% Al alloy aged between 240–360° C, the '*a*' and '*c*' lattice parameters of the f.c. tet. martensite increased and decreased respectively. This change corresponded to a 2% volume reduction. At the same time the microhardness increased from approximately 450 to 900 kg mm^{-2}. Furthermore, Ni_3Al was detected on ageing at 400° C, from X-ray powder photographs. It was concluded that precipitation of a metastable form of NiAl had occurred. In specimens aged above 700° C Shklyar *et al.* [4] and Arkhangel'skaya *et al.* [3] observed that Ni_3Al formed. Russell and Edington showed that on ageing Ni–36 at.% Al at 875° C, Ni_3Al was formed both as irregular rods and as grain boundary film.

The purpose of this work is to study the precipitation mechanisms in martensite during ageing of nickel rich NiAl.

2. Experimental procedures

A ternary alloy, Ni–30.3 at.% Al–6.6 at.% Cr, was studied. This alloy was prepared by argon arc melting, encapsulation in mild steel and extrusion at 1100° C. Discs were cut from the extruded material by spark machining and were solution treated at 1300° C in pure argon or in a vacuum of 10^{-5} torr. Specimens were water quenched from the solution treatment temperature and then aged in pure argon or in a vacuum of 10^{-5} torr. After ageing, specimens were water quenched Thin foils were prepared by electropolishing in a Fischione "Twin Jet Electropolisher" using a solution of 5% perchloric acid in ethanol, maintained at −30° C with an applied voltage of 50 V. The thin foils were then examined in a JEM 200A electron microscope.

3. Results

The precipitation mechanism was dependent on the ageing temperature, different mechanisms being observed below and above a temperature of approximately 700° C.

---

* Present address: Central Electricity Generating Board, South Eastern Region, Suffolk Road, Gravesend, Kent, UK

3.1. Ageing below 700° C

The quenched alloy is martensitic [2]. The martensite plates are internally twinned in {101} ⟨101⟩ (Enami *et al.* [5], Moskovic [2]). Moskovic [2] has proposed a superordered structure for martensite. The sequence of events observed on ageing over the temperature range 515 to 650°C is

(1) G.P. zone-like plates → (ii) f.c. tet. precipitates → (iii) ordered Ni_3Al.

The G.P. zone-like plates form during the quench as described previously [2]. Ageing at 595°C does not modify the martensite structure but leads to the formation of metastable precipitates in martensite. Fig. 1 shows a diffraction pattern for the aged condition, with $[\bar{1}1\bar{1}]$ matrix beam direction. In addition to the fundamental spots there are two different kinds of superlattice spots: A- arises from the superordered structure of the matrix and B- corresponds to precipitate superlattice spots. The crystal structure and lattice parameters of the matrix and Ni_3Al precipitates were determined from the selected area diffraction patterns. Indexed diffraction pattterns are shown in Fig. 2. The martensite matrix is b.c. tet. with lattice parameters $a = 2.55$ Å, $c = 3.19$ Å and $c/a = 1.25$; whilst the precipitates are f.c. tet. with lattice parameters $a = 3.52$ Å, $c = 3.26$ Å and $c/a = 0.927$. The precipitates have an ordered structure comparable to the Ni_3Al fcc LI_2 structure. The orientation relationship between the precipitates and the matrix can be described by the transformation matrices:

$$\begin{bmatrix} h \\ k \\ l \end{bmatrix}_{\text{precipitate}} = \begin{bmatrix} 110 \\ \bar{1}10 \\ 001 \end{bmatrix} \begin{bmatrix} h \\ k \\ l \end{bmatrix}_{\text{matrix}}$$

for crystallographic planes, and

$$\begin{bmatrix} u \\ v \\ w \end{bmatrix}_{\text{precipitate}} = \tfrac{1}{2} \begin{bmatrix} 110 \\ \bar{1}10 \\ 002 \end{bmatrix} \begin{bmatrix} u \\ v \\ w \end{bmatrix}_{\text{matrix}}$$

for crystallographic directions.

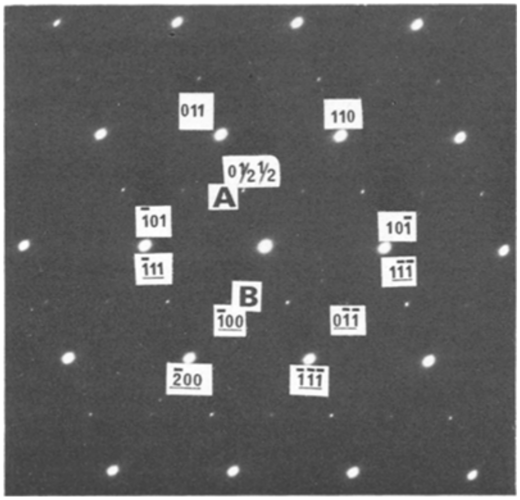

Figure 1 Diffraction pattern taken from material aged at 595° C. $[\bar{1}\,1\,\bar{1}]_{NiAl} \| [0\,1\,\bar{1}]_{Ni_3Al}$ beam direction.

The precipitate morphology was determined from bright and dark field images, using incident beam directions close to ⟨111⟩, [110], [010] and [100] matrix zone axes. The projected particle shapes are either approximately circular or elliptical and are shown in the table. The major axis of the ellipse was always along the trace of the twins within the martensite plates. These results are consistent with an ellipsoidal particle with major axis in the twin plane. An approximate trace analysis combined with the observation of maximum projected ellipticity for a ⟨112⟩ viewing direction, indicates that the long axis is within ±20° or ⟨112⟩.

Fig. 3 shows precipitate size as a function of ageing time. Two dimensions of the ellipsoid, equatorial radius '*a*' and polar radius '*c*', are plotted. The precipitate size can be compared with the twin size and spacing which may be estimated from the selected area diffraction pattern and centred dark field respectively. In the diffraction pattern (Fig. 4a) the twin reflections are in the form of streaks, indicating that the twin plates are only a few atomic spacings thick. The dark field micrograph (Fig. 4b) obtained with twin reflection marked A in Fig. 4a, shows the spacing of twin plates to be approximately 60 to 300 Å. The smallest precipitate dimension '*a*' is thus always larger than the thickness of the twin plate and is in many instances larger than the twin plate spacing. Therefore the growing precipitate particle must interact with the twin plates. Two forms of interaction have been observed as shown in Fig. 5. In Fig. 5a precipitates grow from the twin plate into the matrix, developing a curved interface by pushing forward the twin boundaries. Consequently, in the dark field micrograph (Fig. 5a) obtained from a twin spot, with electron beam parallel to the composition plane, the twin plates are swollen. In Fig. 5b precipitates grow

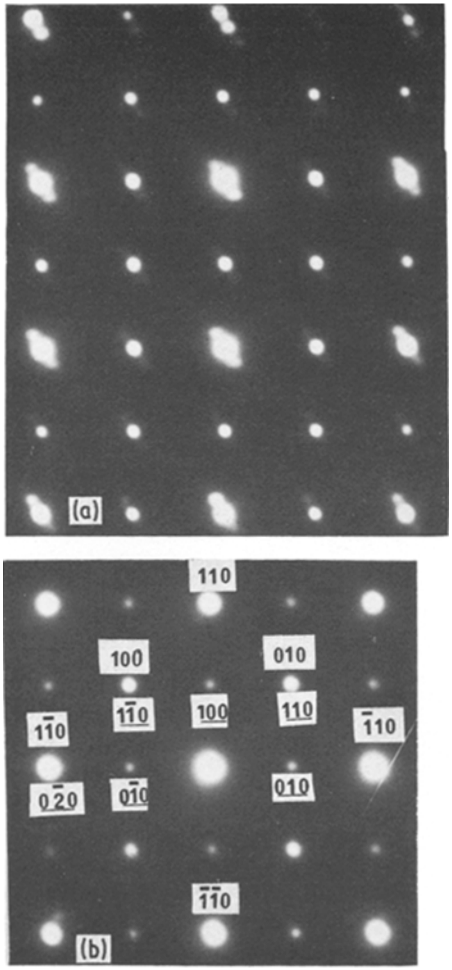

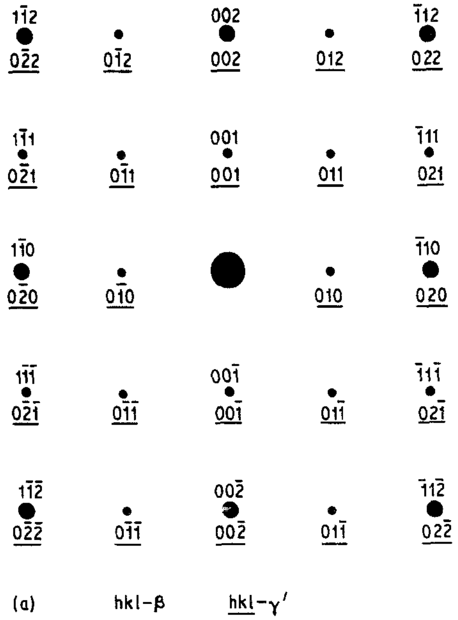

Figure 2 Diffraction patterns taken from material aged at 595° C. Beam directions are paralled to (a) $[\bar{1}\,\bar{1}\,0]_{\text{NiAl}} \| [\bar{1}\,0\,0]_{\text{Ni}_3\text{Al}}$ and (b) $[0\,0\,1]_{\text{NiAl}} \| [0\,0\,1]_{\text{Ni}_3\text{Al}}$. Streaking is due to internal twinning in the martensite.

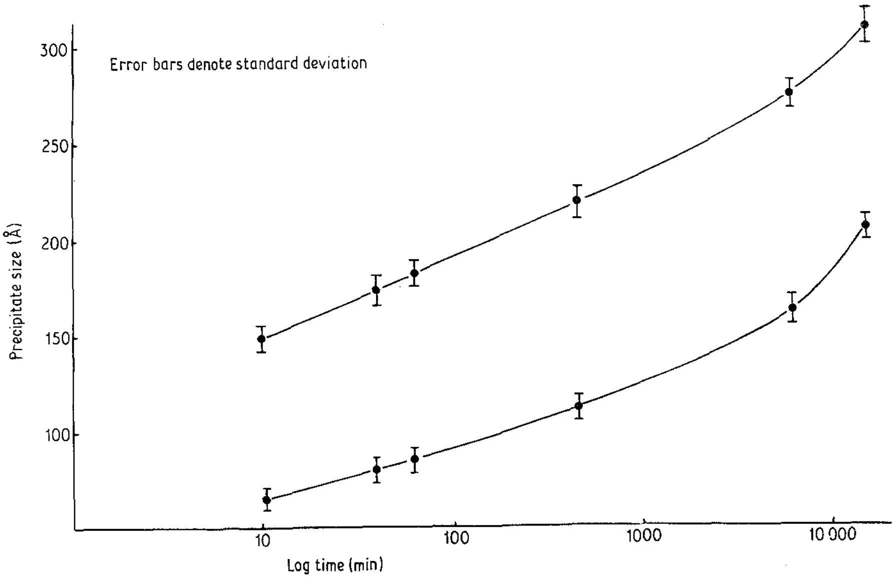

Figure 3 Variation of precipitate size with ageing time at 595° C. *c* and *a* are the semiaxes of the ellipsoid.

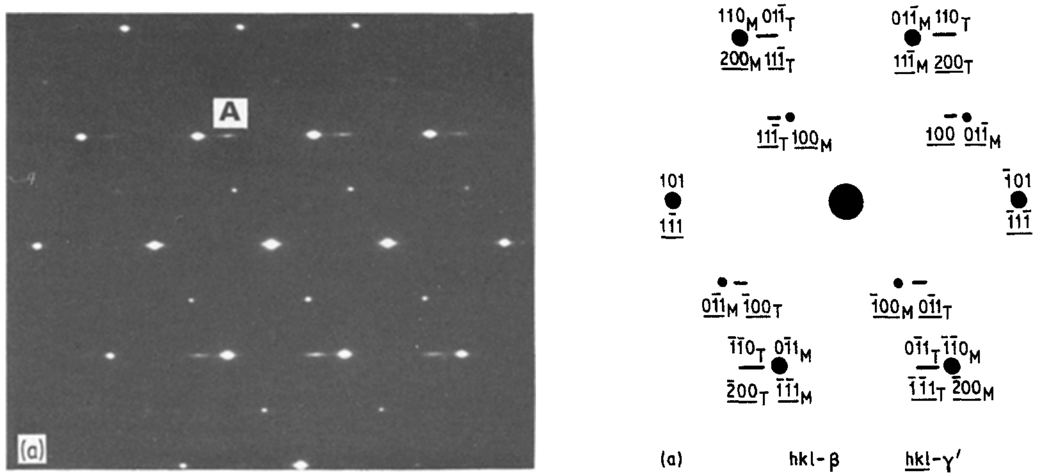

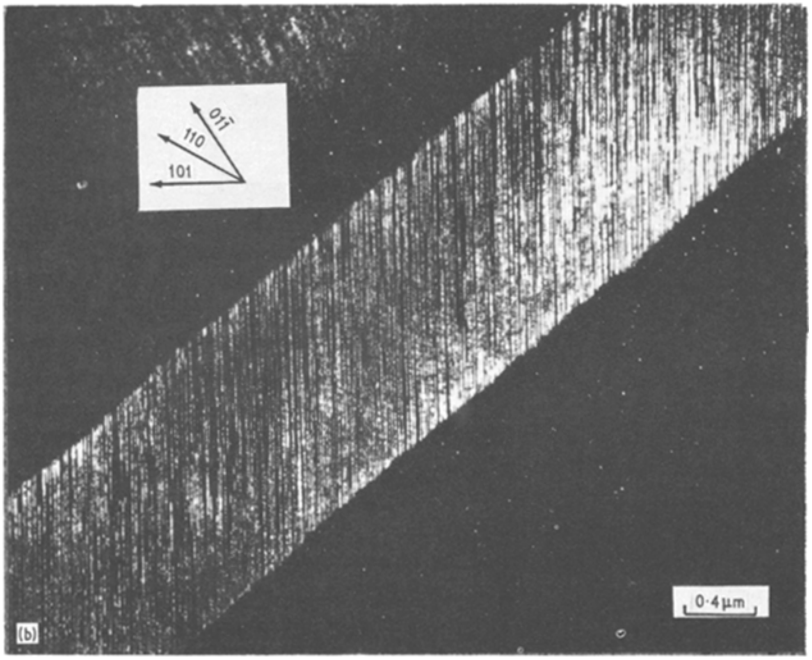

Figure 4 (a) Selected area diffraction pattern for the $[\bar{1}11]_{\mathrm{NiAl}} \| \langle 011 \rangle_{\mathrm{Ni_3Al}}$ beam direction and (b) centered dark field.

from the matrix into the twin plate. Precipitates follow the orientation of the matrix, and all the interfaces are coherent. In Fig. 5b precipitates can be seen either to develop growth twins, or to cut up the twins which then become discontinuous

3.2. Ageing above 700° C

The sequence of events on ageing at 750, 850, 950 and 1000° C can be described as follows:

(i) G.P. zone-like precipitates (as quenched condition)

(ii) heterogeneously nucleated ordered f.c. tet. Ni_3Al $c/a = 0.976$

(iii) gradual change of $c/a \rightarrow 1$

(iv) ordered cubic LI_2 Ni_3Al

The G.P. zone-like precipitates, which formed during quenching from the solution treatment temperature, dissolve. Ni_3Al precipitates then nucleate heterogeneously at grain boundaries, on the interface between martensite plates (marked A in Fig. 6) and on the twins within the martensite plates (marked B in Fig. 6).

The precipitates inside laths are rod shaped and are parallel to the (101) twinning plane. Interface precipitates have an irregular shape. Very fine faults are initially present in Ni_3Al precipitates (Fig. 7), but these anneal out during ageing. The nature of these faults could not be determined because of complex diffraction effects. With either increased ageing time or temperature the interface

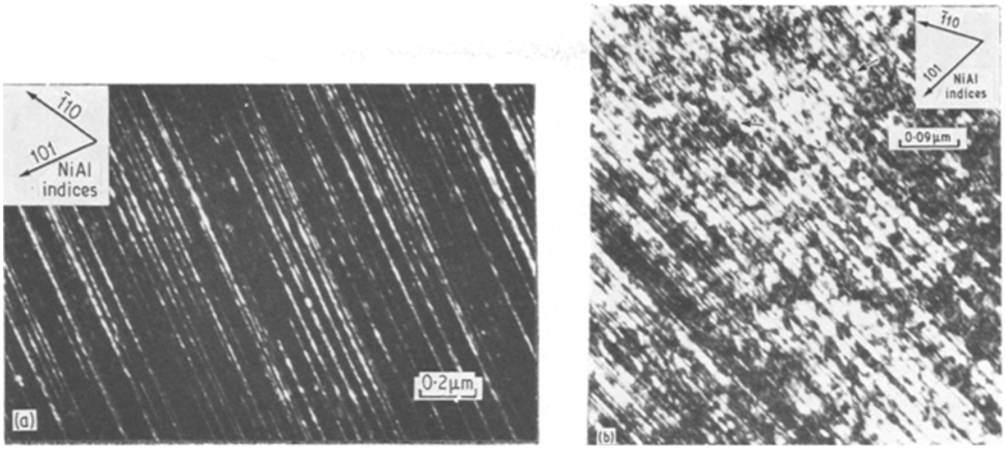

Figure 5 (a) Dark field image using the twin reflection. Twin plates appear swollen due to the precipitates. (b) Bright field image. Internally twinned precipitates and twin cutting may be observed, although this effect is masked by high density of precipitates.

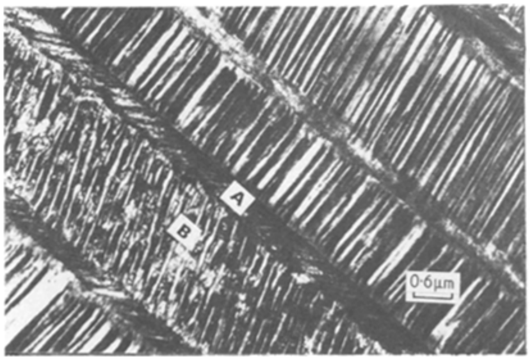

Figure 6 The precipitates after ageing for 10 min at 850° C. Nucleation of the precipitates on the interface between two martensite laths A and on the microtwins inside the laths B.

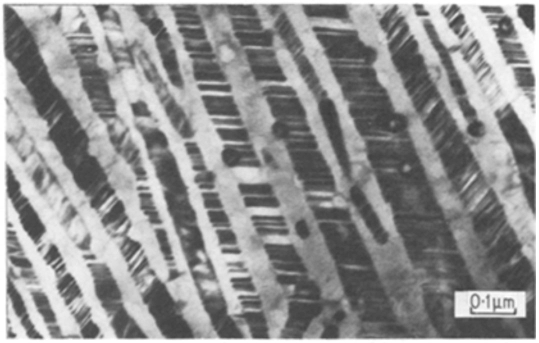

Figure 7 Bright field electron micrograph showing heavily faulted Ni_3 3Al precipitates after 10 min ageing at 750° C.

nucleated precipitates grow at the expense of the twin nucleated form. The resulting microstructure is similar to that reported by Russell and Edington [1], for the Ni–36 at.% Al alloy aged at 875° C, and consists of Ni_3Al laths and grain boundary film in a NiAl matrix. The matrix contains fine G.P. zone-like precipitates that form during quenching from the ageing temperature.

The crystal structure of the precipitate showed a gradual transition from the ordered f.c.tet. form described above, to an equilibrium cubic form with $a_{\gamma'} = 3.35$ Å, which was present typically after 2h at 850° C. There was an accompanying change in the matrix from b.c.tet, with $a = 2.56$ Å, $c = 3.2$ Å and $c/a = 1.25$, to the equilibrium cubic B2 form with $a = 2.68$ Å. At no time in the aged condition were the b.c.o. or 'super-ordered' forms of martensite, described by Moskovic [2], detected.

The orientation relationship between the Ni_3Al and the NiAl matrix is:

$$\{0\,1\,1\}_{NiAl} \parallel \{1\,1\,1\}_{Ni_3Al} \quad \text{for planes,}$$

$$\langle 1\,1\,\bar{1}\rangle_{NiAl} \parallel \langle 1\,0\,\bar{1}\rangle_{Ni_3Al} \quad \text{for directions,}$$

during all stages of ageing. In the early stages of ageing the matrix and precipitates are twin related: compare Figs. 8a and b which are taken from NiAl and Ni_3Al twin related spots in the $[\bar{1}\,1\,1]$ matrix zone axis (Fig. 8c).

4. Discussion

4.1. Ageing below 700° C

Two events occurred during ageing below 700° C. The first step, the formation of G.P. like zones during quenching, has been discussed by Moskovic [2]. The growth of f.c.tet. Ni_3Al precipitates during ageing will be discussed here. The growth of

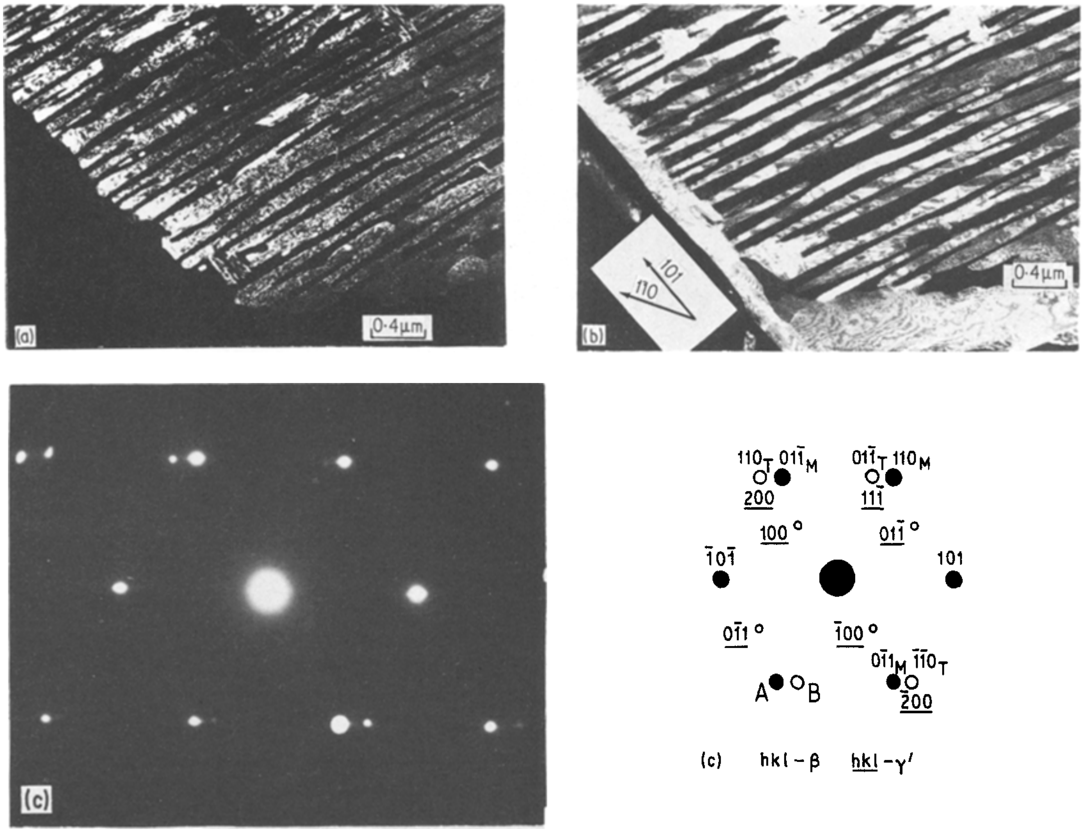

Figure 8 Material aged for 10 min at 850° C, dark field images using a matrix reflection marked A (a) precipitate relection marked B (b), selected area diffraction pattern with a twin symmetry $[\bar{1}\,1\,1]_{\mathrm{NiAl}} \parallel [0\,1\,1]_{\mathrm{Ni_3Al}}$ (c).

these precipitates involves interaction between the precipitate particles and microtwins, though this phenomenon is not common for coherent precipitation. A model for precipitate growth in martensite will now be proposed.

Motion of a dislocation with Burgers vector 1/6 ⟨1 1 2⟩ on {1 1 1} in Ni_3Al leads to a complex fault involving the creation of both a stacking fault and an antiphase domain boundary (Kear *et al.* [6]). In a single complex stacking fault, $AB\underline{CA}/CABC$, the two layers $\underline{C}\ \underline{A}$ constitute a twin. Such a monolayer fault can be produced by the dislocation mechanism proposed by Cottrell and Bilby [7] and extended by Venables [8] to account for the production of multilayer faults which form a microtwin. The effective stress on dislocations, during the formation of a twin by the Venables mechanism, comes from the chemical driving force. Because of the orientation relationship between the NiAl and Ni_3Al precipitate, the {1 1 1} ⟨1 1 2⟩ twin shear in the precipitate is also a twin shear on {1 0 1} ⟨$\bar{1}$ 0 1⟩ in the matrix. Consequently the Ni_3Al can twin to correspond with the transformation twin in the NiAl matrix.

A growing Ni_3Al precipitate can interact with microtwins in two ways:

(1) When a precipitate particle encounters a twin interface, the particle twins and the twin interface will be inside the particle. In this case the precipitate remains coherent with the matrix.

(2) A growing precipitate encountering a twin boundary pushes it forward so that the interface becomes curved and coherency is lost. The twin interface will now coincide with the interface between the precipitate and the matrix.

Both situations are depicted in Fig. 9. Which of the two processes occurs will depend on the energies involved in each case. The two situations shown in Fig. 9 will now be compared. On the matrix side, the particle energies are the same for both cases,whilst on the twin side, the particle energies are different in each case. In the first case

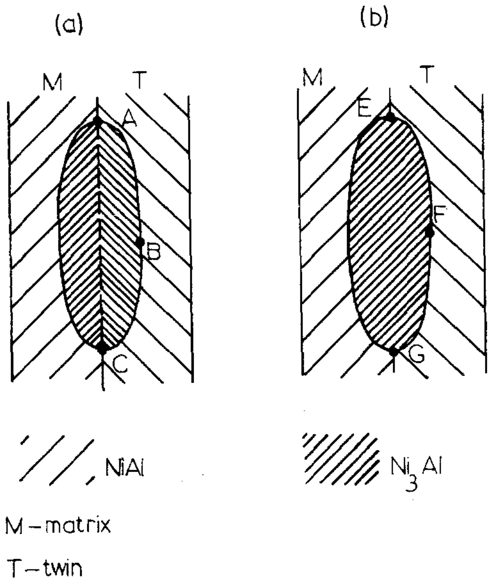

Figure 9 Two possible modes of precipitate twin interaction (a) precipitate twins, (b) twin interface bulges forward.

(Fig. 9a) the precipitate particle has twinned and now contains a precipitate twin boundary. Thus the energy of the particle on the twin side has two terms, γ_1* and γ_2; where γ_1 is the energy term associated with a precipitate twin boundary (AC in Fig. 9a), this being the stacking fault energy of a complex Ni_3Al fault, and γ_2 is the surface energy of the coherent interface (ABC in Fig. 9a). In the second case, Fig. 9b, the particle has not twinned and becomes incoherent on the twin side. The surface energy γ_3 of an incoherent particle interface (EFG in Fig. 9b) contains contributions from the matrix twin energy γ_4 (γ_4 is different from γ_1), an energy term γ_5 which accounts for the dislocations which are required to untwin the matrix, and an energy term γ_6 arising from the composition and ordering differences between NiAl and Ni_3Al.

The configuration in Fig. 9a will have a lower energy than that in Fig. 9b when $\gamma_1 A_T + \gamma_2 A_p < \gamma_3 A_p$, where A_T is the area of the precipitate twin interface and A_p is that of the precipitate-matrix interface. This condition may always be satisfied since $\gamma_3 A_p > \gamma_1 A_T$ and $\gamma_2 A_p$ is very small. Initially, however, the growing particle will push the matrix–twin interface forward until there is enough free energy in the system to generate the dislocations required to twin the particle and transform it into the configuration in Fig. 9a. The dislocations required to twin the particle are already present in the interface because the twin direction and plane in the particle and matrix are parallel as a result of the orientation relationship between two phases.

The precipitate-twin interaction will have two consequences:

(1) An Ni_3Al particle that starts to grow from the matrix may push the twin interface sufficiently far forward to cut through the twin before there is enough energy available to twin the particle. Thus the twins, which are relatively thin, will become chopped up during precipitate growth.

(2) An Ni_3Al particle that starts to grow from the twin will first push the twin boundary forward and produce the effect shown in Fig. 5a. Continued growth will eventually twin the particle which then reverts to the configuration in Fig. 9a. This configuration corresponds with the internally twinned particle in Fig. 5b.

The precipitate growth will involve two steps: the concentration of Ni at the interface increases by diffusion, and subsequently the precipitate interface moves forward by shear processes. The former will be the rate controlling process.

4.2. Ageing above 700° C

Observations of heterogeneous nucleation of the precipitate above 700° C imply that the G.P. zones have dissolved. The twin like relation between the precipitates and the matrix, shown in Fig. 10, implies that these precipitates nucleate on the microtwins. The second nucleation site, which appears to be the martensite plate interface, is easily understood because it is effectively similar to a grain boundary. The rapid growth of the precipitate formed at the martensite plate interfaces probably reflects conventional ripening combined with possible increased mobility of and diffusion at these interfaces. The lenticular morphology of the Ni_3Al particles formed above 700° C is a result of either the best matching between $\{1\,1\,0\}_{NiAl}$ and $\{1\,1\,1\}_{Ni_3Al}$ planes or the relative mobility of the various interfaces as proposed by Aaronson [9].

5. Conclusions

(1) Coherent matrix precipitation of a metastable form of Ni_3Al occurs below 700° C.

(2) Precipitate growth in martensite involves a particle-twin interaction, which can take two

---

[*] $\gamma_1, \gamma_2, \gamma_3, \gamma_4, \gamma_5, \gamma_6$ are energies per unit area

forms: either the particle can push forward the twin interface, which then becomes curved, or the particle is developing growth twins.

(3) A model in which twins in Ni_3Al are generated by Venables mechanism is proposed to account for these observations.

(4) Above 700° C, heterogeneous precipitation of Ni_3Al occurs on twins within and at the interface between martensite plates.

(5) The orientation relationship in the equilibrium structure between Ni_3Al precipitates and NiAl matrix is

$$\{1\,1\,1\}_{\mathrm{Ni_3Al}} \parallel \{0\,1\,1\}_{\mathrm{NiAl}}$$

$$\langle 1\,0\,1\rangle_{\mathrm{Ni_3Al}} \parallel \langle 1\,1\,\bar{1}\rangle_{\mathrm{NiAl}}$$

Acknowledgements

The author would like to thank Professor J.W. Edington for helpful discussions, Professor R.W.H. Honeycombe for the provision of Laboratory facilities and International Nickel Limited for supplying the material. This work has been carried out with the support of Procurement Executive, Ministry of Defence.

References

1. K. C. RUSSELL and J. W. EDINGTON, *Metal Science Journal* **6** (1972) 20.
2. R. MOSKOVIC, *J. Mater. Sci.* **12** (1977) 489.
3. A. A. ARKHANGEL'SKAYA, I. N. BOGACHEV, V. V. A. LITVINOV and YE G. PANTSYREVA, *Fiz. Metal. Metalloved* **34** (1972) 541.
4. R. S. SHKLYAR, V. S. LITVINOV and YE G. PANTSYREVA, *ibid* **32** (1971) 181.
5. K. ENAMI, S. NENNO and K. SCHIMIZU, *Trans. Jap. Inst. Metals,* **14** (1973) 161.
6. B. H. KEAR, G. R. LEVERANT and J. M. OBLAK, *Trans. ASM* **62** (1969), 639.
7. A. H. COTTRELL and B. A. BILBY, *Phil. Mag.* **42** (1951) 573.
8. J. A. VENABLES, Deformation Twinning, Proceedings of Conference Sponsored by Met. Soc. AIME (Gordon and Breach, New York, 1964).
9. H. I. AARONSON, "Decomposition of Austenite by Diffusional Processes", (Wiley, New York, 1962) p. 387.

Received 23 August and accepted 9 December 1976.